J. Fluid Mech. (2009), *vol.* 634, *pp.* 419–431.
doi:10.1017/S0022112009007976 Printed in the United Kingdom

Origins of radiometric forces on a circular vane with a temperature gradient

NATHANIEL SELDEN[1], CEDRICK NGALANDE[1], NATALIA GIMELSHEIN[2], SERGEY GIMELSHEIN[2]† AND ANDREW KETSDEVER[3]

[1]University of Southern California, Los Angeles, CA 90089, USA
[2]ERC Incorporated, Edwards AFB, CA 93528, USA
[3]University of Colorado at Colorado Springs, Colorado Springs, CO 80933, USA

(Received 24 March 2009 and in revised form 30 April 2009)

Radiometric force on a 0.12 m circular vane is studied experimentally and numerically over a wide range of pressures that cover the flow regimes from near free molecular to near continuum. In the experiment, the vane is resistively heated to about 419 K on one side and 394 K on the other side, and immersed in a rarefied argon gas. The radiometric force is then measured on a nano-Newton thrust stand in a 3 m vacuum chamber and compared with the present numerical predictions and analytical predictions proposed by various authors. The computational modelling is conducted with a kinetic approach based on the solution of ellipsoidal statistical Bhatnagar–Gross–Krook (ES-BGK) equation. Numerical modelling showed the importance of regions with elevated pressure observed near the edges of the vane for the radiometric force production. A simple empirical expression is proposed for the radiometric force as a function of pressure that is found to be in good agreement with the experimental data. The shear force on the lateral side of the vane was found to decrease the total radiometric force.

1. Introduction

When a thin vane is immersed in rarefied gas, and a temperature gradient is imposed between the two sides of the vane either resistively or radiatively, a force will generally be exerted that will tend to move the vane from the hot to the cold side. Such a force is conventionally called radiometric, as it is identified with the forces acting in the Crookes radiometer (Crookes 1874; Loeb 1961). There has been little controversy regarding the cause of the radiometric forces at very low pressures since the explanation proposed by Tait & Dewar (1875). Here, the forces are due to molecules leaving the hotter surface with higher velocities than those leaving the colder one. This results in a pressure imbalance across the two surfaces, with the resultant net force in the direction from hot to cold.

The well-known free molecular expression may be used for the radiometric force in the case of the gas mean free path is much larger than the radiometer size (Passian

† Email address for correspondence: gimelshe@usc.edu

et al. 2002),

$$F = \frac{p}{2} A \left(\sqrt{\frac{\alpha_E T_h + (1-\alpha_E) T_g}{T_g}} - \sqrt{\frac{\alpha_E T_c + (1-\alpha_E) T_g}{T_g}} \right), \tag{1.1}$$

where T_h and T_c are the hot and the cold temperatures, respectively, T_g is the free stream gas temperature, A is the area of the radiometer and α_E is the energy accommodation coefficient. Generally, the energy accommodation coefficients may be different on different sides of the vane.

While the issue is settled for the free molecular flow, the sources of the radiometric forces at higher pressures are much less transparent, which has created a number of controversies in the past (Loeb 1961). Even today, the issues does not seem to be fully settled (Scandurra, Iacopetti & Colona 2007). It is important to note, however, that many of the explanations are based on a phenomenon called thermal transpiration (Loeb 1961), which was first explained by Reynolds.

The consequence of this explanation has been a number of radiometric force theories proposed over the years. One of the most rigorous explanations was proposed by Maxwell (1879) and later improved by Hettner & Czerny (1924). This explanation contends that fluid particles will move from the cold side of the vane to the hot side. The reaction to this flow current is a force on the vane towards the cold side. The region where this force is observed is therefore the lateral sides of the vane. The tangential force of reaction on the vane per unit area is (Hettner & Czerny 1924)

$$F = \frac{3}{4} \frac{\eta^2}{a \rho T} \frac{\partial T}{\partial x}, \tag{1.2}$$

where η is the coefficient of viscosity, ρ is the density, a is the distance to the opposite vane (or, generally, to the chamber walls), T is the temperature and x is the length along the axis chosen parallel to the temperature gradient. Hettner and Czerny's force calculations compared favourably to earlier calculations by Knudsen who studied radiometric forces at higher pressures. The Hettner and Czerny's calculations were successful in explaining the radiometric forces in different settings. Using these calculations, it was possible to explain the Rubens and Nichols radiometers (Rubens & Nichols 1897). Their calculations were also extended to specify radiometric forces in other geometries including spheres. This analysis agreed with that of Sexl (1926) who independently investigated a case of an ellipsoid of rotation and later a sphere. These theories have also been successful in explaining photophoresis.

Einstein (1924) published a paper putting forward a theory of radiometric force. His theory, as with the Hettner and Czerny calculations, is based on some elements of the thermal transpiration phenomenon. According to the Einstein's derivation, the force acting on the vane perimeter,

$$F = p \lambda \frac{\Delta T}{T}, \tag{1.3}$$

where p is gas pressure, λ is the gas mean free path, ΔT is the temperature difference and T is the absolute temperature. The force in (1.3) is produced in an area that is one mean free path thick, and is given per unit length of the edge. This theory found partial confirmation in the experiments by Marsh (1926). Later, Sexl showed that Einstein's theory was deduced from a reasoning which was not strictly accurate; he modified the theory and derived an expression for the radiometric force on a dish

radiometer (Sexl 1926) as

$$F = \frac{14.72}{n+5}\frac{p\lambda^2}{T}\Delta T, \tag{1.4}$$

where n is the number of active internal degrees of freedom of gas molecules (0 for a monatomic gas). The main difference between Sexl and Einstein's formulas is that Sexl's radiometric force is inversely proportional to gas pressure while Einstein's force is independent of pressure and is proportional to the perimeter of the vane. Even though there is a pressure term in (1.3), this term cancels out with the mean free path term and becomes a constant independent of pressure (Loeb 1961). It must also be emphasized that (1.3) assumes the radiometric force to act only within a single mean free path from the edge.

A general expression that is consistent with the bell-shaped dependence of the radiometric force on pressure, consistent with many experimental studies was proposed by Westphal (1920), $F \propto \frac{p}{a} + \frac{1}{bp}$, where a and b are geometry and gas dependent constants. Note that the interest in radiometric phenomena significantly reduced after 1930s, but started to grow rapidly in the last decade, primarily because radiometric phenomena were found to be useful in a number of different micro- and large-scale devices. One of the most important of these is atomic force microscopy (AFM), a research field that, although invented back by Binning, Quate & Gerber (1986), has been brought to the forefront of modern nanotechnologies in the last several years (see, for example, Giessibl 2003; Gotsman & Durig 2005; Hinterdorfer & Dufrne 2006). The use of radiometric forces as an approach to study gas-surface translational energy accommodation has been suggested by Passian *et al.* (2003). Gas flow around a laser opto-microengine was examined with the direct simulation Monte Carlo (DSMC) method by Ota, Nakao & Sakamoto (2001). The DSMC method was also used by Selden *et al.* (2009), where the effect of the vane geometry on the radiometric force production was studied both numerically and experimentally. A new concept of a high-altitude aircraft supported by microwave energy that uses radiometric effects has also been put forward by Benford & Benford (2005).

Most recently, (Scandurra *et al.* 2007) have derived a new expression for radiometric force that has both pressure and shear components. For the normal force per unit area on a thin vane, they obtained

$$F_n = (2-\alpha_E)\frac{15k}{32\sqrt{2}\pi\sigma^2}\Delta T l, \tag{1.5}$$

where α_E is the energy accommodation coefficient, k is the Boltzmann constant, $\pi\sigma^2$ is the total collision cross section and l is the vane perimeter. For the shear force per unit area, the expression is

$$F_\tau = \alpha_E\frac{15k}{64\sqrt{2}\pi\sigma^2}\frac{\Delta T}{\lambda}(\tau l), \tag{1.6}$$

where τ is the vane thickness. One of the key assumptions of this work is constant pressure in the gas surrounding the heated vane.

It is important to note that aside from the expression for the free molecular flow regime, practically all analytical estimates of the radiometric force were implicitly or explicitly assuming a collision-dominated flow, where the radiometer vane area is much larger than the gas mean free path. This is essentially a slip flow regime, where the impact of the free-molecular, area dominated forces is relatively small. This explains that the proposed expressions depend on the perimeter of the radiometer

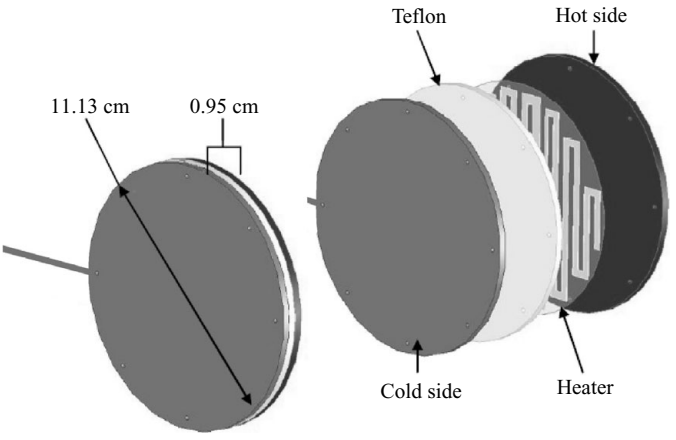

FIGURE 1. CAD drawing of the radiometric device.

vane, and not on its area. While this is a reasonable approach for many cases where the velocity distribution function is close to equilibrium and the pressures at the centres of two sides of the radiometer are equilibrated, it is not obvious that such an approach is applicable to the regime where the flow is far from equilibrium, and both the area and the edge contribute to the radiometric forces. Note that it has been shown recently by Selden *et al.* (2009) that in the range of pressures where the radiometric force is maximum, both area and edge driven forces are important.

The main objectives of this work are the experimental and numerical study of the accuracy of different estimates of the radiometric forces at a range of pressures where the force is near its maximum, the analysis of the pressure gradients near the radiometer vane and the evaluation of the associated edge and shear effects and their relative importance in the radiometric forces. Direct experimental measurements of a force on a resistively heated aluminium vane immersed in argon gas are conducted in the pressure range where the force is near its maximum. The measurements are complemented by numerical modelling that is based on a kinetic approach, namely a solution of the ellipsoidal statistical Bhatnagar–Gross–Krook (ES-BGK) model kinetic equation, which allows detailed analyses of gas flow near the vane and surface force distributions. Qualitative analysis of the edge force mechanisms allowed the authors to propose a simple empirical expression for a quick estimate of the radiometric forces.

2. Experimental set-up and numerical approach

To study the effects of the argon gas pressure on the production of radiometric forces on a vane, a circular plate device was used. The device consisted of a Teflon insulator placed between two aluminium plates, with each plate having a thickness of 0.318 cm. A resistive heater was affixed between one of the aluminium plates and the Teflon insulator, and the entire device was assembled using eight low-conductivity nylon machine screws with 2.13 mm diameters. The assembled device has a total thickness of 0.95 cm, with a diameter of 11.13 cm and is shown in figure 1. The radiometer was mounted on a modified version of the nano-Newton thrust stand (nNTS) (Jamison, Ketsdever & Muntz 2002) located inside the 3.0 m diameter vacuum chamber. More detail on the thrust stand is given by Selden *et al.* (2009).

The experimental data was obtained by evacuating the chamber to a base pressure below 10^{-3} Pa. A constant voltage was applied to the heater, and this resulted in the

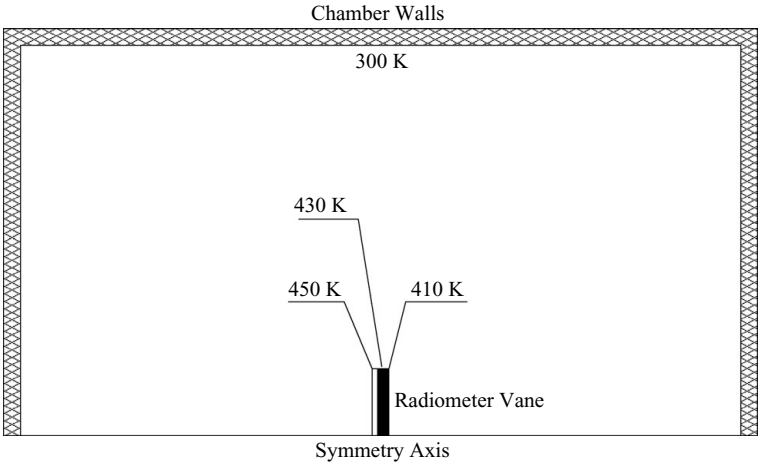

FIGURE 2. Computational set-up.

main surfaces reaching temperatures of approximately 419 K (hot) and 394 K (cold). The background pressure inside the chamber was varied by filling the chamber with argon over a range of pressures from 0.1 to 1.0 Pa. Note that using argon gas in this work allowed the authors to avoid ambiguities associated with the internal degrees of freedom and internal energy relaxation of molecular gases. The experimentally measured force was normalized by the temperature difference between the hot and cold plates, ΔT, for the purpose of comparing results for different pressures and chambers. Verification of the validity of the experimental normalization method is demonstrated by Selden *et al.* (2007), where exceptional linearity with temperature difference is observed.

A finite volume solver solution of model kinetic equations (SMOKE) developed at ERC Inc. has been used to deterministically solve the ellipsoidal statistical (ES) model kinetic equation described by Holway (1966) (called ES-BGK hereafter to emphasize its connection to the original Bhatnagar-Gross-Krook equation of Bhatnagar, Gross & Krook 1954). SMOKE is a parallel code based on conservative numerical schemes developed by Mieussens (2000). The code has both two-dimensional and axisymmetric capabilities. A second-order spatial discretization is used along with implicit time integration. Fully diffuse reflection with complete energy accommodation is applied at the vane and chamber walls. A symmetry plane (symmetry axis in axisymmetric computations) was set at the lower boundary. Two computational domains have been used, $0.44\,\mathrm{m} \times 0.22\,\mathrm{m}$ (two-dimensional) and $3\,\mathrm{m} \times 1.5\,\mathrm{m}$ (axisymmetric). For the smaller domain, a smaller (0.039 m high) vane was used. The use of the smaller domain allowed modelling of radiometric flows at very low Knudsen numbers (below 0.01), while the use of the larger domain allowed for direct comparison with the experimental data. Hereafter, Knudsen numbers are calculated as the ratio of the gas mean free path in the free stream (undisturbed flow far from the radiometer) to the diameter of the vane. The gas mean free path is evaluated with a VHS/VSS model expression given by (4.65) in Bird (1994). The grid convergence was achieved by increasing the number of spatial nodes and points in the velocity space. The latter one was (18,18,12) for the results presented below, and the number of spatial cells varied from 5000 to 50 000 depending on the chamber size. The temperature and geometric set-up is illustrated in figure 2. Note that the temperature of the lateral side of the vane is set as a piecewise constant with three different temperature

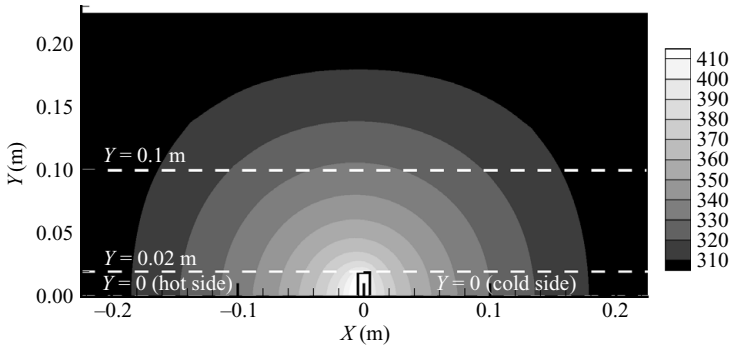

FIGURE 3. Temperature field (K) around the radiometer vane 2 Pa.

values (cold side temperature, hot side temperature and the average between them). This is a reasonable approximation of a three-layer geometrical set-up used in the experiments. No special numerical adjustment has been made to account for the temperature discontinuity at the surface, and no numerical instabilities related to the discontinuities have been noticed in the computations. The radiometric force on the vane was calculated through the integration of the velocity distribution functions of the incoming and outgoing molecules. Both the normal component of molecular velocities on the working sides of the vane (pressure) and the tangential component of velocities on the lateral side of the vane (shear) contribute to the total radiometric force, and were therefore computed.

3. Results and discussion

Consider first the numerical solution obtained in a small chamber for an argon pressure of 2 Pa. The temperature field for this case is presented in figure 3. For this intermediate Knudsen number, about 0.07, there is a noticeable temperature jump at the heated radiometer vane surfaces, which exceeds 10 K at the centre of the vane. Such a temperature jump may be expected for the Knudsen number under consideration. The temperature then quickly decreases to its free stream value of 300 K, with the rate of decrease being approximately the same in all directions. The quantitative behaviour of the gas temperature is shown in figure 4 where the temperature profiles are presented along the dashed lines plotted in figure 3. The temperature gradient is highest at the centre of the vane ($y = 0$) on both hot and cold sides, which differs somewhat from the assumption made in the theoretical model developed by Scandurra *et al.* (2007). There, the gradients along the lateral side of the vane were assumed to be stronger than those near the centre due to a thin vane geometry.

Another important assumption made by Scandurra *et al.* (2007) is that of a constant pressure near the radiometer vane. A close-up view of the pressure field in the vicinity of the radiometer is given in figure 5. The lower half of the flow is a mirror of the upper half; it is shown to provide a better picture of the flow. The conclusion here is that not only the pressure is different at the cold and hot sides of the vane, as well as along the lateral sides, but also that the pressure changes along both the hot and the cold sides. There are regions of high pressure being formed near the edges of the vane. Even though the gas pressure in these regions ($Y \sim 0.015$ m and $Y \sim -0.015$ m) is only about 0.5 % larger than the corresponding values near the centre ($Y \sim 0$), this difference is close to the difference between the pressure near the hot and cold sides

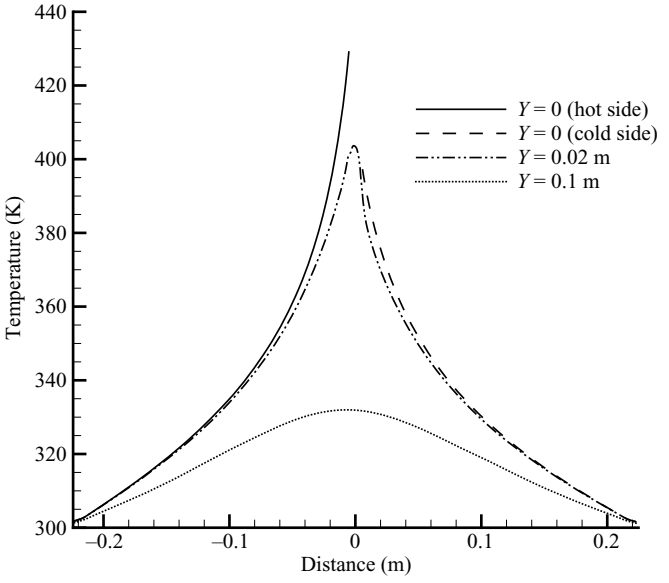

FIGURE 4. Temperature profiles along different cross-sections parallel to the symmetry axis.

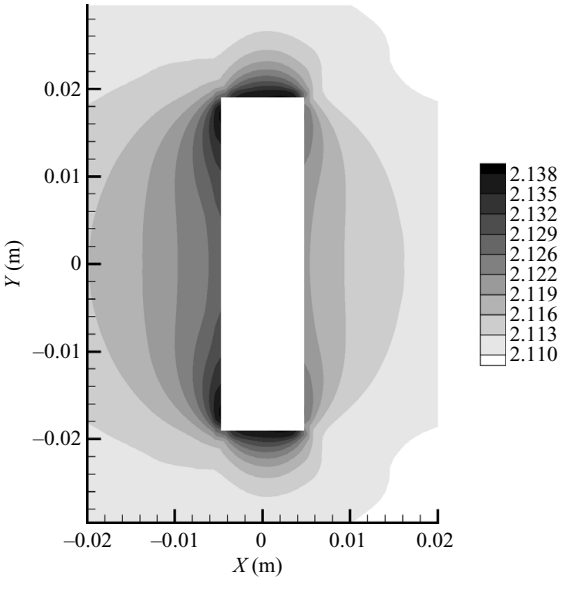

FIGURE 5. Pressure distribution (Pa) around the vane.

for any given value of Y between −0.019 and 0.019 m. Therefore it is critical for the radiometric force production.

Figure 6 shows the computed distribution of the surface pressure difference between the hot and the cold sides for different gas pressures in two-dimensional case (i.e. in effect the pressure component of the radiometric force). The pressure difference, that is uniform for a free molecular flow, is still nearly constant along the vane for a pressure of 0.305 Pa (Knudsen number about 0.4). For a pressure of 1.219 Pa, for which the radiometric force is close to maximum, there is a visible difference between

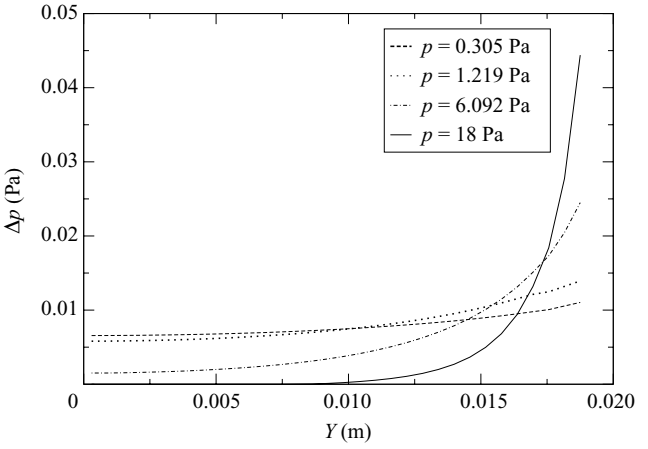

FIGURE 6. Surface pressure difference between the hot and the cold sides of the vane for various gas pressures.

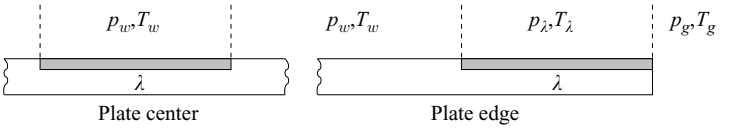

FIGURE 7. Schematics of the gas conditions near the radiometer vane.

the force production near the centre and near the edge, with the latter being about two times larger. The difference sharply increases with pressure, and at 18 Pa there is no force production in the central part of the vane (the pressure is equilibrated between the hot and the cold sides). Most of the force is created within about ten mean free paths from the outer edges of the vane.

The computations clearly show that, for a collisional flow, the force on the working side of the vane reaches its maximum near the edge. The formation and the existence of this maximum may be qualitatively explained as follows. Let us analyse the molecular fluxes on the two small regions, each with the size equal to the gas mean free path near the vane edge λ, and the mean free path is assumed to be significantly smaller than the vane size. One of these regions is located near the centre of the vane, and the other is adjacent to the vane edge, as schematically shown in figure 7. Consider first the region located near the centre of the vane. The flux on this region is determined by the gas conditions above it (between the dashed lines) as well as the gas conditions to the left and to the right of this region, as molecules coming on the surface may cross the dashed lines. Since the gas mean free path is small compared to the vane size, the gas conditions (both pressure and temperature) above the central region and to the sides of it are approximately the same, and may be denoted as p_w and T_w, respectively.

The bulk flow velocity near the vane is very small in radiometric flows, and its contribution to the total pressure on the working side of the vane is negligible. For molecules impinging on the surface, the inward number flux on the central region may generally be written as

$$\dot{N} = n_w \int_{-\infty}^{\infty} \int_{-\infty}^{\infty} \int_{0}^{\infty} c_x f_w \mathrm{d}c_x \mathrm{d}c_y \mathrm{d}c_z. \tag{3.1}$$

Here, c_x is the velocity in the direction normal to the vane, c_y and c_z are the tangential velocities and n_w and f_w are the number density and the velocity distribution function of gas near the central region. When the gas is close to equilibrium, the number flux on a stationary vane may be approximated as an expression for an equilibrium stationary gas (see, for example, (4.24) in Bird 1994) $\dot{N} \approx n\bar{c}/4$, where $\bar{c}$ is the mean molecular speed.

The principal difference between the central and edge regions in terms of the inward number flux is that for the latter this flux is determined not only by gas state immediately above the vane but also by gas to the right of the vane. In this area, the gas has pressure p_g and temperature T_g. Whereas the pressure is expected to be close to the pressure near the surface, $p_g \approx p_w$, the temperature there is obviously lower, $T_g < T_w$. Let us denote the temperature ratio R, $R = T_g/T_w < 1$. Since the pressure values are approximately the same, the number density ratio will then be $n_g/n_w = R^{-1} > 1$. Then the ratio of the number fluxes based on molecules coming to the central and edge regions from the right may be approximated as $\dot{N}_g^{right}/\dot{N}_w^{right} \approx R^{-\frac{1}{2}} > 1$. Therefore, while initially the momentum fluxes on the central and edge regions may be similar, the number flux on the edge region is larger. Since molecules are assumed to undergo complete momentum and energy accommodation on the surface, such an inequality in number fluxes results in a slight increase in pressure near the edge of the vane. The reflected molecules may generally collide with the incoming molecules, and be directed back to the surface. Due to the molecular collisions between the incoming and outgoing molecules, such an increase in pressure eventually causes a higher momentum flux on the edge.

Note that since the relaxation scale of the translational mode amounts to several mean free paths, the actual size of the edge region with elevated pressure is larger than a single mean free path. This qualitative analysis is expected to be applicable to some extent even for cases when mean free path is comparable to the size of the vane. For many radiometric devices, the maximum force is observed at a Knudsen number about 0.1. For flows at Knudsen numbers close to this value, the contribution of the edge forces is expected to be fairly large, and comparable to that of the area forces Selden *et al.* (2009). Obviously, with the increase of gas pressure and decrease in the Knudsen number the surface area where the edge-related radiometric force is significant will decrease, since it is proportional to the gas mean free path. An effective area may therefore be introduced for a circular vane as

$$A = \pi R_{eff}^2 = \pi R^2 - \pi(R - n\lambda)^2, \tag{3.2}$$

where R is the vane radius, λ is the mean free path of the ambient gas and $n\lambda$ specifies the thickness of the edge area where the force is produced. This effective area, when plugged into the free molecular expression (1.1), may be used for an evaluation of the radiometric force. Note that in the limit of $\lambda \to 0$ the force predicted with this expression becomes independent of pressure, similar to (1.3).

If an assumption similar to Einstein's is made, and $n = 1$ is used, the radiometric force computed with a simple empirical expression (1.1)–(3.2) gives surprisingly close agreement with the present experimental results, as shown in figure 8. It is interesting to note that the assumption of $n = 1$ works very well, even though it has been shown above that the pressure imbalance occurs over a region of ten mean free paths. The agreement is fairly good in the free molecular and nearly free molecular flows (pressures below or about 0.1 Pa, or Knudsen numbers above 0.5) that are characterized by a nearly linear increase in the radiometric force, and the area related radiometric forces are dominant. Even though the present empirical expression stems

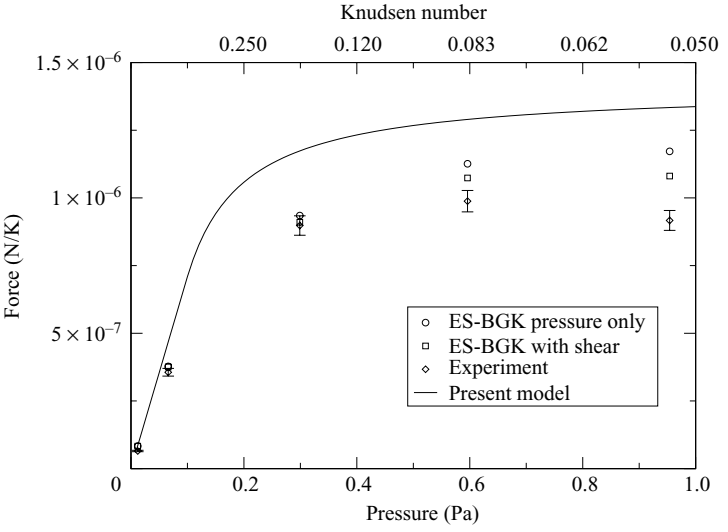

FIGURE 8. Experimental and calculated force on the vane for different pressures.

from the free molecular formula, the agreement is also quite reasonable in the transitional flow where the collisions start to reduce the radiometric force, and both area and edge related radiometric forces are important (Knudsen numbers between 0.5 and 0.05, where the maximum radiometric force is observed).

Note that the main reason for the overprediction of the experimentally observed radiometric force by the empirical expression (1.1)–(3.2) appears to be the assumption of the fully diffuse reflection on the radiometer surface used here. Obviously, using a lower value of the accommodation coefficient – and there is an indication (Saxena & Joshi 1989) that this coefficient may indeed be lower – will correspondingly decrease the predicted force. Note also that (3.2) applied for a circular radiometer may be easily modified for any other geometrical shape. Comparison with recent results of Selden *et al.* (2009) shows a similarly reasonable agreement of expression (1.1)–(3.2) with the experimental data for a smaller circle, while for the rectangular geometry it overpredicts the data near the force maximum by about a factor of two.

Figure 8 also presents the results of the numerical solution of the ES-BGK equation (the large domain case is presented here). Two sets of data points are given: (i) the full radiometric force that include both pressure force on the working side of the vane and the shear force on the lateral side of the vane, (ii) the radiometric force without the shear. The full radiometric force is somewhat larger than the experimental data due to several reasons. First, and most important, the actual surface accommodation both on the vane and on the chamber walls is not fully diffuse. An accommodation coefficient lower than unity will obviously decrease the computed force value. Second, the ES-BGK equation is an approximation to the Boltzmann equation, the most general equation that describe dilute gas flows, and its solutions may deviate somewhat from the solution of the full Boltzmann equation. Third, there are uncertainties inherent both in the experimental (estimated to be up to 4 %) and numerical (up to 3 %, based on the convergence patterns and the estimation of the numerical parameter effects) modelling results.

Analysis of the ES-BGK results shows that the combined shear force is acting towards the reduction of the total radiometric force, contrary to what was previously

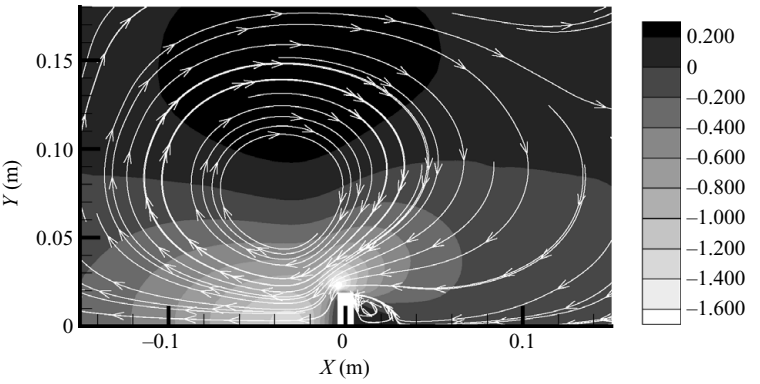

FIGURE 9. Velocity field (m s^{-1}) and streamlines around the radiometric vane 2 Pa.

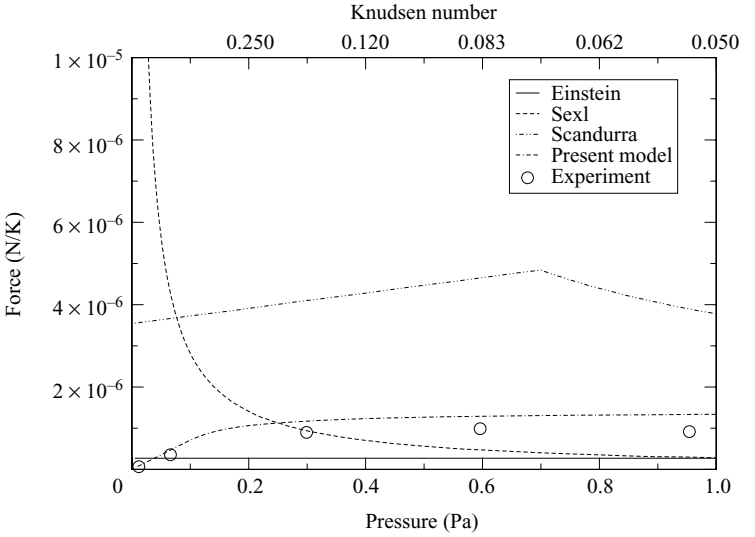

FIGURE 10. Force prediction according to different models.

assumed by several authors (Hettner & Czerny 1924; Scandurra *et al.* 2007). The shear force is practically non-existent at the lowest pressures under consideration, but increases to almost 8 % for the pressures where the force is near its maximum. Note that the authors have validated this fact with additional simulations using the DSMC method, a statistical approach to the solution of the Boltzmann equation. The DSMC computations also resulted in a shear force acting opposite to the pressure force. The negative shear force may be explained when considering the ES-BGK distribution of flow velocities and streamlines, shown in figure 9 in the vicinity of the vane for a chamber pressure of 2 Pa and the small domain case. The temperature gradients generate two counter-propagating vortices in the upper half of the flow, a very large vortex centred above the vane closer to the hot side, and a much smaller vortex adjacent to the cold side. Among the sources that create these vortices may be the local pressure maxima near the edges of the vane, that move gas towards the centre both at the cold and hot sides. The larger vortex creates a combined force on the lateral side of the vane that is directed from cold to hot side. Finally, figure 10 presents the comparison of the radiometric force estimates obtained using

analytical expressions proposed by different authors, with the present experimental data. Although the expression of Sexl (1926) does not capture the correct trend for smaller pressures, it still produces a reasonable estimate for pressures that correspond to the maximum force in the experiment. The expression of Scandurra *et al.* (2007) significantly overpredicts the experimental data, and the expression of Einstein (1924) underpredicts the maximum force.

4. Conclusions

An experimental and computational study of the radiometric force has been performed for an argon gas in a wide range of pressures. Accurate measurements of the radiometric force on a resistively heated 0.12 m diameter circular vane were conducted with a nano-Newton thrust stand in a 3 m vacuum chamber for pressures between 0.01 and 1 Pa. A kinetic approach based on the solution of the ES-BGK equation has been applied to numerically analyse the radiometric flow for pressures from 0.01 to 18 Pa.

The numerical results demonstrated the existence of regions with elevated gas pressure. A qualitative explanation of the formation of these regions is given and a simple expression that allows a quick estimate of the radiometric force as a function of pressure is suggested. The force predictions obtained with this expression are in a good agreement with the experimental data. The ES-BGK results somewhat overpredict the experimental data, which is primarily attributed to the fully diffuse energy accommodation used in the calculations.

The force production was found to be nearly constant along the vane for pressures smaller than those where the force is maximum, and strongly shifted towards the edge for higher pressures. Generally the region of the force production was about ten mean free paths thick. The shear force exerted on the lateral side of the radiometer vane was found to decrease the total radiometric force. Finally, various expressions for the radiometric force, suggested in literature, were evaluated through the comparison with the experimental data. The present model gives reasonable agreement with experimental data for the pressure regime were both area and edge related contributions to the radiometric force are important, and the radiometric force is near its maximum.

The work at USC and ERC was supported in part by the Propulsion Directorate of the Air Force Research Laboratory at Edwards Air Force Base, California. The work at ERC was supported by AFOSR. The authors thank Dr Ingrid Wysong and Dr E. P. Muntz for many fruitful discussions.

REFERENCES

Benford, G. & Benford, J. 2005 An aero-spacecraft for the far upper atmosphere supported by microwaves. *Acta Austonaut*. **56**, 529–535.

Bhatnagar, P. L., Gross, E. P., Krook, M. 1954 A model for collision processes in gases I: small amplitude processes in charged and neutral one-component systems. *Phys. Rev.* **94**, 511–525.

Binning, G., Quate, C. F. & Gerber, C. H. 1986 Atomic force microscope. *Phys. Rev. Lett*. **56**, 930–933.

Bird, G. A. 1994 *Molecular Gas Dynamics and the Direct Simulation of Gas Flows*. Clarendon Press.

Crookes, W. 1874 On attraction and repulsion resulting from radiation. *Phil. Trans. R. Soc. Lond.* **164**, 501–527.

Einstein, A. 1924 Zur theorie der radiometrerkrafte. *Zeitschrift fur Physik* **27**, 1–5.

Giessibl, F. 2003 Advances in atomic force microscopy. *Rev. Mod. Phys.* **75** (3), 949–983.

Gotsman, B. & Durig, U. 2005 Experimental observation of attractive and repulsive thermal forces on microcantilevers. *Appl. Phys. Lett.* **87**, 194102.

Hettner G. & Czerny, M. 1924 The measurement of the thermal slip of gases. *Zeitschrift fur Physik* **30**, 258–267.

Hinterdorfer, P. & Dufrne, Y. F. 2006 Detection and localization of single molecular recognition events using atomic force microscopy. *Nat. Methods* **3**, 347–355.

Holway, L. H. 1966 Numerical solutions for the BGK-model with velocity dependent collision frequency. In *Proceedings of Fourth International Symposium on Rarefied Gas Dynamics, University of Toronto, Toronto, 1964* (ed. J. H. D. Leeuw), pp. 193–215. Academic Press.

Jamison, A. J., Ketsdever, A. D. & Muntz, E. P. 2002 Gas dynamic calibration of a nano-Newton thrust stand. *Rev. Sci. Instrum.* **73** (10), 3629–3637.

Loeb, L. B. 1961 *The Kinetic Theory of Gases*. Dover, pp. 364–386.

Marsh, H. E. 1926 Further experiments on the theory of the vane radiometer. *J. Opt. Soc. Am.* **12**, 135–148.

Maxwell, J. C. 1879 On stresses in rarified gases arising from inequalities of temperature. *Phil. Trans. R. Soc. Lond.* **170**, 231–256.

Mieussens, L. 2000 Discrete-velocity models and numerical schemes for the Boltzmann–BGK equation in plane and axisymmetric geometries. *J. Comput. Phys.* **162** (2), 429–466.

Ota, M., Nakao, T. & Sakamoto, M. 2001 Numerical simulation of molecular motion around laser microengine blades. *Math. Comput. Simul.* **55**, 223–230.

Passian, A., Warmack, R. J., Ferrell, T. L. & Thundat, T. 2003 Thermal transpiration at the microscale: a Crookes cantilever. *Phys. Rev. Lett.* **90** (12), 124503.

Passian, A., Wig, A., Meriaudeau, F., Ferrell, T. L. & Thundat, T. 2002 Knudsen forces on microcantilevers. *J. Appl. Phys.* **92** (10), 6326–6333.

Rubens H. & Nichols, E. F. 1897 Ueber das verhalten des Quarzes gegen Strahlen grosser Wellenlnge. *Annalen der Physik und Chemie* **60**, 418–462.

Saxena, S. C. & Joshi, R. K. 1989 *Thermal Accommodation and Adsorption Coefficients of Gases*. Hemisphere Publishing.

Scandurra, M., Iacopetti, F. & Colona, P. 2007 Gas kinetic forces on thin plates in the presence of thermal gradients. *Phys. Rev.* E **75**, 026308.

Selden, N., Ngalande, C., Gimelshein, S. & Ketsdever, A. 2007 Experimental and computational observation of radiometric forces on a plate. *Paper 2007-4403*. AIAA.

Selden, N. Ngalande, C. Gimelshein, S., Muntz, E. P., Alexeenko, A. & Ketsdever, A. 2009 Area and edge effects in radiometric forces. *Phys. Rev.* E **79**, 041201.

Sexl, T. 1926 The theory of radiometer effects II. *Annalen der physik* **81** (24), 800–806.

Tait, P. G. & Dewar, J. 1875 Charcoal vacua. *Nature* **12**, 217–218.

Westphal, W. H. 1920 Messungen am radiometer. *Zeitschrift fur Physik* **23**, 92–100.